ENGEVISTA

Página da revista: http://www.uff.br/engevista/seer/

Use of Fe$_2$O$_3$-TiO$_2$ in solar photo-Fenton process for the phenol degradation

Jerlan Alves da Silva
Gessyca Borges dos Santos
Vivian Stumpf Madeira
Maria Luisa de Almeida Ramalho
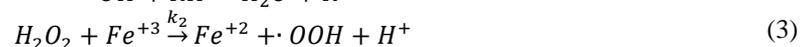Islanny Larissa Ouriques Brasileiro
Arthur Marinho Cahino

Abstract: In this work a Fe$_2$O$_3$-TiO$_2$ catalyst, at the proportion 60:40 (%mass), was produced using a modified Pechini method. The catalyst was characterized and used in the degradation of phenol in aqueous solution through a solar photo-Fenton reaction. Experiments were performed varying the concentration of H$_2$O$_2$, catalyst, phenol, and pH of the aqueous solution, in order to determine the reaction rate and propose a mechanism. Characterization showed the presence of Fe$_2$O$_3$ and anatase and rutile phases of TiO$_2$. Pseudobrookite (Fe$_2$TiO$_5$) was also found in the material. The Fe$_2$O$_3$-TiO$_2$ catalyst presented higher efficiency (90% of phenol removal) and degradation rate than the two isolated oxides in the process photo-Fenton heterogenous in optimum conditions. The proposed mechanism shows that the union of the two oxides, Fe$_2$O$_3$ and TiO$_2$, facilitates the reduction and oxidation reactions of Fe^{+2}/Fe^{+3} and Ti^{+4}/Ti^{+3}, increasing the amount of surface OH groups and consequently the catalytic activity.
Keywords: Effluent treatment, Phenol, photo-Fenton, catalysts, Iron oxides, Sunlight.

1. Introduction

Water scarcity is one of humanity's greatest challenges. Industrial processes involving large volumes of water are especially damaging to the environment due to the large-scale contamination of water (ZENG *et al.*, 2011; XU *et al.*, 2012). The scientific community has been absorbing more work in optimization of the effluents treatment that have high number of organic compounds due to the need to preserve natural resources and to make industrial processes sustainable. Phenol is a corrosive, toxic and carcinogenic organic compound that is generally present in refinery and petrochemical wastewaters, also present in chemical operations and plastic industry (VIRARAGHAVAN AND ALFARO, 1998). Titanium dioxide (TiO_2) is used as a catalyst in photocatalytic processes due to its chemical stability, non-toxicity, possibility of immobilization in solids and great efficiency in the degradation of pollutants, but its application in processes activated by sunlight is limited, since its absorption range is in the UV spectrum (MAHADIK *et al.*, 2014). The mixing of TiO_2 with other materials has been used as a way to overcome this limitation and its work can be found in the literature (PENG *et al.*, 2010; LI *et al.*, 2014; MENDONÇA *et al.*, 2014). The hematite (Fe_2O_3) is an iron oxide that has considerable relevance in this area being a promising photocatalyst, because it has lower bandgap and its interaction with TiO_2 has already been proved positive in other works (AKHAVAN AND AZIMIRAD, 2010; AMBATI AND COGATE, 2017; MISHRA AND CHUN, 2015).

The Advanced Oxidation Processes (AOPs) aim the generation and use of the hydroxyl radicals ($\cdot OH$), a strong oxidizing agent with extremely high kinetics constant (10^8-10^{11} $M^{-1}s^{-1}$), in the degradation of toxic organic compounds, such as phenol (BOKARE AND CHOI, 2014). The Fenton system is one of these processes and the degradation of the organic compound is achieved by the $\cdot OH$ attack, generated by the reaction between Fe^{+2} and H_2O_2 (Equations (1) and (2)). At low pH, the soluble Fe^{+3} is reduced to Fe^{+2}, by H_2O_2 (Equation (3)). As the rate of oxidation reaction of Fe^{+2} to Fe^{+3} is much faster (k_1=51 $M^{-1}s^{-1}$ and k_3=0.001-0.01 $M^{-1}s^{-1}$), at any instant time in the system there is an excess of Fe^{+3} compared to Fe^{+2}. Therefore, a more efficient catalytic system should increase the rate of reduction of Fe^{+3} to Fe^{+2}, regenerating the reduced species, to the Fenton reaction (LIANG *et al.* 2017). The UV-light irradiation in the Photo-Fenton process achieves this goal, with the Photo-reduction of Fe^{+3} to Fe^{+2} (Equation (4)) and additional generation of hydroxyl radical (DU *et al.*, 2014; DOUMIC *et al.*, 2015).

$$Fe^{+2} + H_2O_2 \overset{k_1}{\to} Fe^{+3} + OH^- + \cdot OH \tag{1}$$

$$\cdot OH + RH \overset{k_2}{\to} H_2O + R \tag{2}$$

$$H_2O_2 + Fe^{+3} \overset{k_2}{\to} Fe^{+2} + \cdot OOH + H^+ \tag{3}$$

$$Fe^{+3}OH^- \overset{light}{\longrightarrow} Fe_i^{+2} + \cdot OH \tag{4}$$

In this work, a Fe_2O_3-TiO_2 mixed oxide catalyst was synthetized, at the proportion 60:40 (%mass) by a modified Pechini method. The objective was achieve and therefore study the synergic effect between Fe and Ti, in the solid phase, for its use in a photo-Fenton process using natural solar light in the degradation of Phenol, by varying the system parameters.

2. Materials and Methods

2.1 Materials

All materials used were of analytical grade. The precursors of metal cations, Ferrous Sulfate ($FeSO_4.7H_2O$) and Titanium Isopropoxide IV ($Ti(OCH(CH_3)_2)_4$) (97%) were purchased from Química Moderna (Brazil) and Sigma-Aldrich (India), respectively. Citric acid and ethylene glycol were purchased from Synth. The water used in the synthesis was distilled.

2.2 Synthesis of mixed oxide Fe/Ti (60:40 mass%) by modified Pechini method

The Fe_2O_3-TiO_2 catalyst was synthesized using a modified Pechini method (PECHINI, 1967) with a citric acid/metal cation ratio of 3:1. The precursors used were Ferrous Sulfate and Titanium Isopropoxide, following a production ratio of 60% Fe_2O_3:40% TiO_2. The pyrolysis was performed in a muffle furnace at 400°C for 1h. The material was de-agglomerated, sifted and then calcined at 500°C for 1 h.

2.3 Characterization of the catalyst

The determination of the phases present in the samples was done by X-ray diffractometry (XRD), obtained with the aid of Bruker D2-Phaser X-ray diffractometer (40 kV and 30 mA), using Cu Kα radiation, in a band of 2Ө. The measurements swept the range between 5° and 80° (2θ), with pitch of 0.02 ° (2θ).

The absorption spectra of the samples were obtained in the medium infrared region in the range of 400-4000 cm^{-1} with a resolution of 4 cm^{-1}. Samples were diluted in KBr at a concentration of approximately 1% by weight. The obtained material was homogenized and hydraulically pressed with 6 tons and the pellets obtained were sent to Perkin Elmer Spectrum-One FT-IR spectrometer, where the spectra were obtained.

The measurement of the specific surface area was done using the Brunauer-Emmet-Teller (BET) method, which is based on the adsorption of a monolayer of an inert gas, usually N_2 or Ar. Micromeritics equipment was used, model Nova 3200 and N_2 gas.

2.4 Evaluation of photocatalytic activity

The photocatalytic tests were performed with the mixed oxide (Fe/Ti) (60:40 %mass) produced by the Pechini method under natural sunlight for the degradation of Phenol. For the tests, phenol solutions were prepared and air inlet (through laboratory pumps) were used. They occurred between the periods of April and May, with exposure to natural sunlight from 10h to

14h. Initially, mixed oxide Fe/Ti, TiO_2 and Fe_2O_3 (all produced by the Pechini method) and a blank sample were tested on the same parameters for comparison between the catalysts. Subsequently, tests were performed using the mixed oxide varying the parameters in each test. There was variation of hydrogen peroxide (H_2O_2), initial solution pH, solids concentration and phenol concentration.

The procedure was carried out in a batch, using a Jar Test, laboratory compressors to supply the air flow and analytical level reagents. The phenol samples were prepared with a concentration of 50 $mg.L^{-1}$, placed under sunlight with mechanical agitation and air flow of 0.5 $L.min^{-1}$ for a period of 3 hours and 30 minutes. Samples were collected at time 0, 10, 30, 50, 80, 110, 160 and 210 minutes, filtered through a microfilter of PVDF membrane to promote separation between the phases. Then, the filtered aliquots were sent for absorbance reading on a UV-Vis scan spectrophotometer (Shimadzu) at 269 nm to obtain their concentration. All graphics were obtained from software Origin Pro 8®.

3. Results and discussion

3.1 Characterization and analysis of the catalyst

The specific surface area calculated for the mixed oxide by the BET method was 59.1693 $m^2.g^{-1}$. Figure 1 (a) shows the XRD analyzes of the samples.
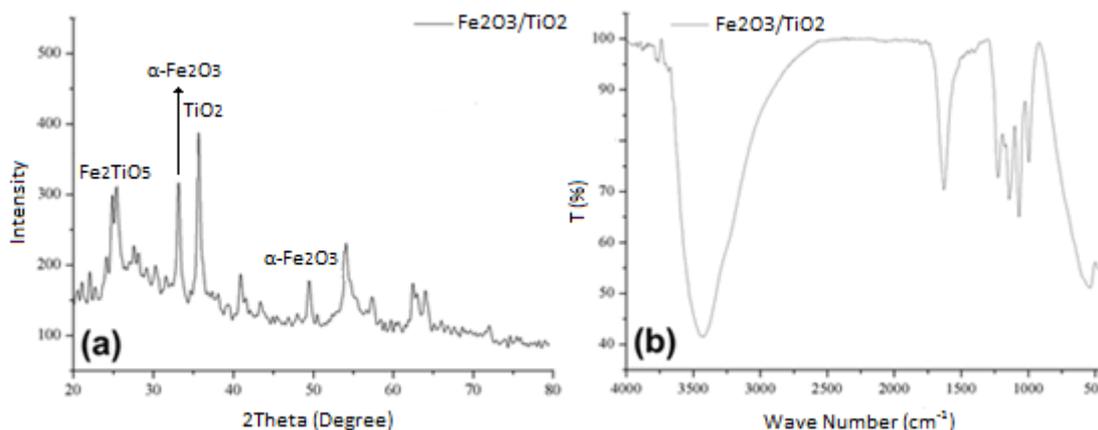
**Figure 1:** (a) X-ray diffraction patterns of Fe_2O_3/TiO_2 and (b) FT-IR spectra of Fe_2O_3/TiO_2

The mixed oxide XRD presents diffraction peaks related to the rhombohedral phase of α-Fe_2O_3 (JCPDS n° 01-1053) and the tetragonal anatase phase of TiO_2 (JCPDS n° 01-0562), a more favorable phase with better photocatalytic properties than the rutile phase. It also presents peaks related to the tetragonal rutile phase of TiO_2 (JCPDS n° 21-1276). It was noticed that some peaks close to α-Fe_2O_3 and TiO_2 may have been superimposed on XRD. The peaks of 25.5° and 32.2° are in accordance with the literature standard (JCPDS n° 20-2302) for

pseudobrookite (Fe_2TiO_5), which is probably formed due to the presence of an iron rich layer on the TiO_2 surface. No considerable peak related to Fe-Ti binding has been observed which may be due to the low intensity of the peaks and/or the formation of small amounts of these phases at the interface between the phases.

Figure 1(b) shows the Infrared Spectra of the samples. The mixed oxide has the presence of the crystalline anatase phase of the titanium dioxide with a lower intensity between 400 and 600 cm^{-1}, which may be related to the overlap with the peak of the hematite at the wave number of 574cm^{-1}. Bands at wavelengths between 3500 and 1600 cm^{-1} indicate humidity in the material. The intense peak around 1050 cm^{-1} is related to the C-O stretch vibration of the precursors used in the synthesis of the material.

3.2 Photocatalytic activity Test

In the first experiment the photocatalytic activity of Fe/Ti mixed oxide (60:40) was evaluated from its performance on phenol degradation compared to titanium TiO_2 and Fe_2O_3 (both produced by the Pechini method) using the following parameters: catalyst concentration of 0.1 $g.L^{-1}$, initial pH of 6.5, initial phenol concentration of 50 $mg.L^{-1}$ and air flow of 0.5 $L.min^{-1}$. In addition, the effect of phenol degradation in the absence of catalyst was also evaluated. In Figure 2 the efficiency were obtained for each catalyst at time intervals of 0 to 210 min.
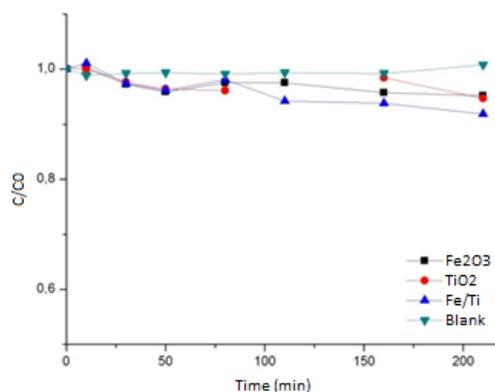

Figure 2: Efficiency for each catalyst at time intervals of 0 to 210 min

It can be observed from Figure 2 that phenol photocatalysis practically did not occur for all the materials used, since the phenol absorption peak did not decrease with time (being similar to the blank test), indicating that the pollutant was not degraded. The phenol removal percentage was 10% for Fe/Ti mixed oxide and 5% for both TiO_2 and Fe_2O_3. It is also possible to observe that there is low adsorption of phenol on the surface of the catalyst, which can be justified due to the low concentration of solids.

3.3 Heterogeneous photo-Fenton test

In the application of the heterogeneous photo-Fenton process, the parameters of the previous experiment were maintained, and the concentration of H_2O_2 added was 100 mg.L^{-1}. Figure 3 shows the UV-Vis absorption spectra of the collected points.
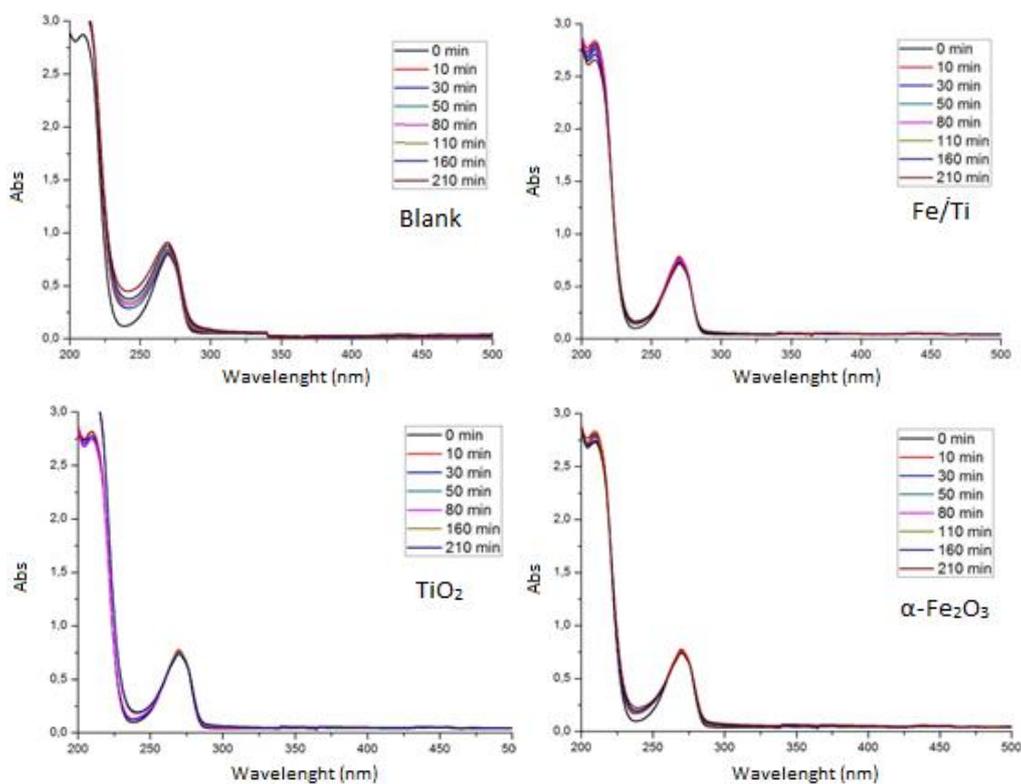
**Figure 3:** Absorption espectra during the heterogeneous photo-Fenton test (C_{H2O2}=100mg.L^{-1}; C_{phenol}=50mg.L^{-1}; $C_{catalystr}$=0.1g.L^{-1} and pH=6.5), with (a) TiO_2, (b) Blank, (c) α-Fe_2O_3 and (d) mixed oxide Fe/Ti

The addition of hydrogen peroxide to the iron, whether in mixed oxide (Fe/Ti) or hematite, radically changes the absorption spectrum of the solution. There is an instantaneous formation of a dark complex with phenol, iron and hydrogen peroxide, with different values of λmax (maximum wavelength), also occurring a color change of the solution, from colorless to yellowish. Furthermore can also be observed that these formed intermediates, which change the absorption spectrum, are degraded.

According to Cong *et al.*, (2012), which also obtained this drastic change in the absorption spectrum, the main intermediates identified in the phenol degradation reaction in the Fenton-type process are benzoquinone, hydroquinone and oxalic acid. A mechanism for degradation of phenol has been proposed, in which, initially, phenol forms benzoquinone and in parallel there is the formation of hydroquinone (which is also transformed into benzoquinone) followed by the breaking of the aromatic ring and total decomposition of the phenol in CO_2 and H_2O.

The phenol degradation kinetics at the 269 nm length are shown in Figure 4. The degradation efficiency of the phenol using hematite was approximately 90%, similar to the mixed oxide Fe/Ti, which was approximately 91%.
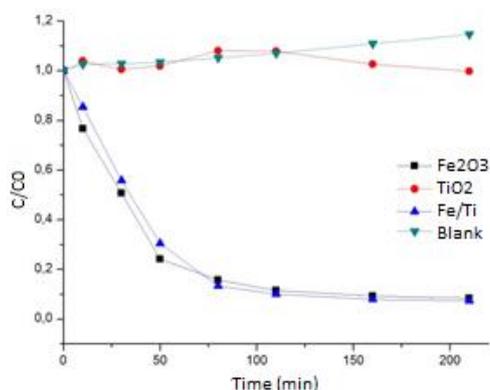

Figure 4: Performance **c**omparison of the mixed oxide, hematite, titanium dioxide and blank (without catalyst). The following initial conditions were used: $C_{H2O2}=100mg.L^{-1}$; $C_{phenol}=50$ mg.L^{-1}; $C_{catalyst}=0.1g.L^{-1}$ and pH$\cong$6.5.

3.3.1 Influence of H₂O₂ concentration

In this test the parameters used were: solution pH=6, phenol concentration 50 mg.L^{-1}, catalyst concentration 0.1 g.L^{-1} and air flow 0.5 L.min^{-1}. H$_2$O$_2$ concentrations were varied from 50 mg.L^{-1} to 200 mg.L^{-1}. The absorption spectra are shown in Figure 5 and Figure 6 shows the degradation kinetics (a) and the relationship between initial velocity and peroxide concentration (b).
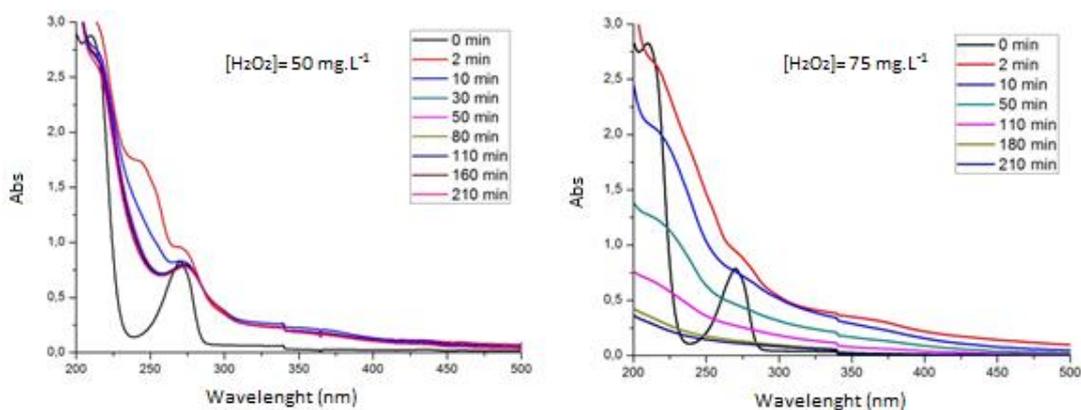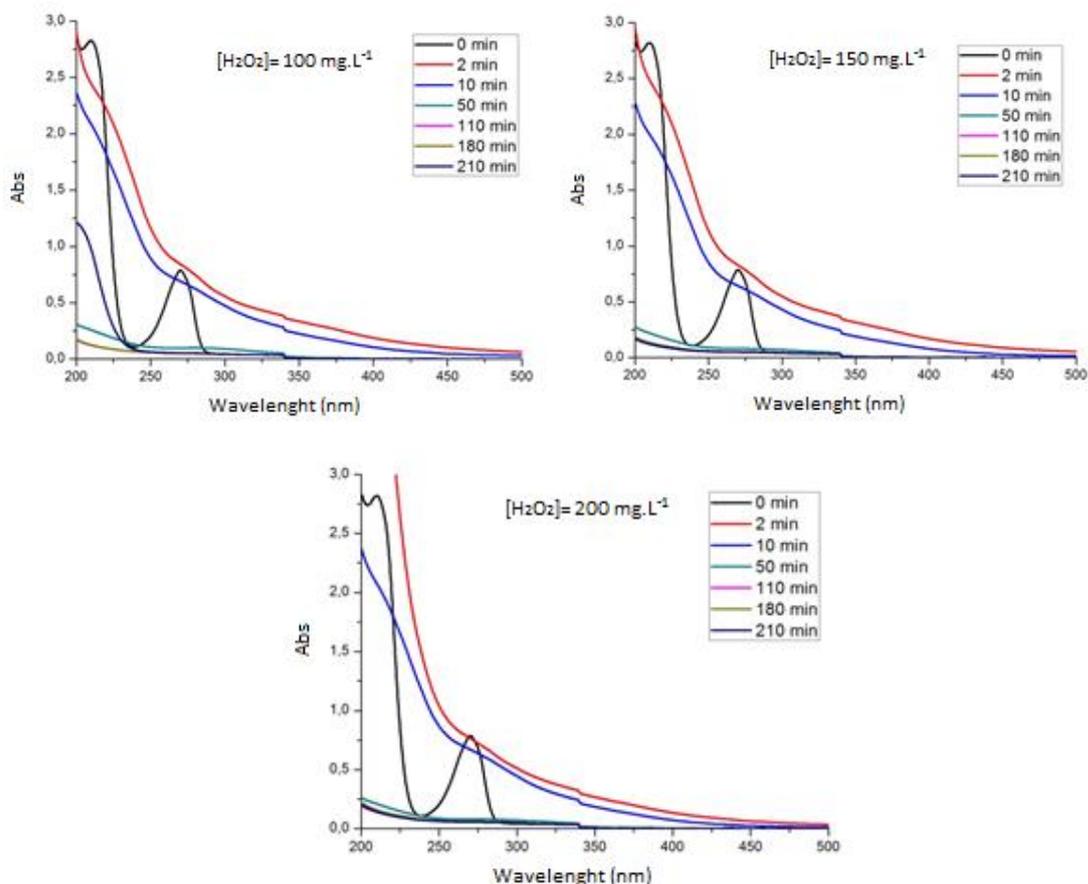
Figure 5: Absorption spectra of phenol solutions during the hydrogen peroxide variation test (C_{phenol}=50mg.L^{-1}; $C_{catalyst}$=0.1g.L^{-1} and pH≅5.8), variating H_2O_2 concentration.
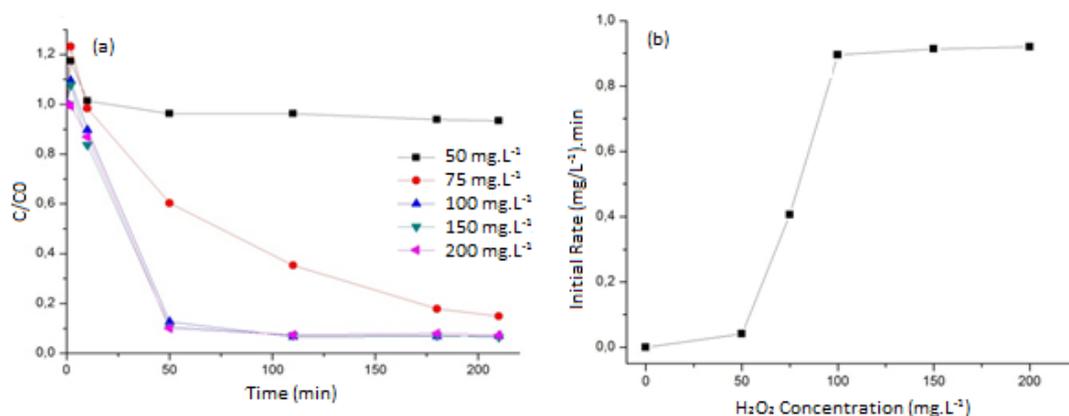
Figure 6: (a) Phenol removal for different H_2O_2 concentrations, with 0.1g.L^{-1} Fe_2O_3-TiO_2, 50mg.L^{-1} phenol, and initial pH=6 and (b) initial rate of reaction *versus* H_2O_2 concentration

For H_2O_2 concentrations above 100 mg.L^{-1}, 90% degradation of the phenol was obtained in 50 min of reaction. At 75 mg.L^{-1}, 80% of phenol degradation was obtained, with a much lower reaction rate. With 50 mg.L^{-1}, almost nothing was removed, however, the formation of intermediates was observed (by the initial absorbance peak, collected in 2 min, and by the scanning spectra obtained for the solution). In a adsorption experiment with phenol and the

764

catalyst, without H_2O_2, after 6.0 hours of contact, the formation of intermediates was also detected.

3.3.2 Influence of initial solution pH

To evaluate the pH interference of the solution in the phenol removal efficiency, a new test was performed by varying the pH from 3.0 to 9.0. The concentration of H_2O_2 used was 100 mg.L^{-1}, the catalyst concentration was 0.1 g.L^{-1} and phenol was 50 mg.L^{-1}. Figure 7 shows the absorption spectra obtained and, in Figure 8, the degradation kinetics for the studied pH range.
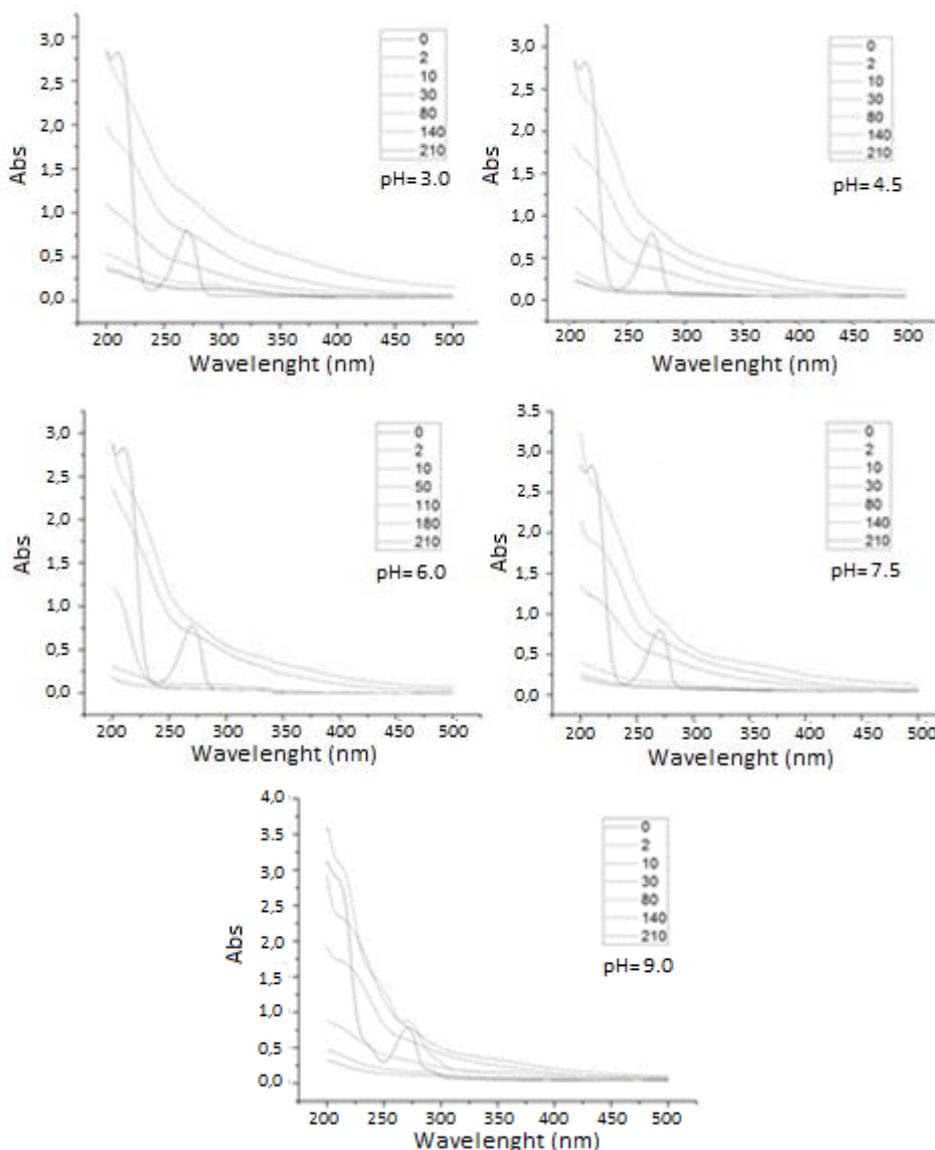
Figure 7: Absorption spectra of phenol solutions during the pH variation test (C_{H2O2}=100mg.L^{-1}, C_{phenol}=50 mg.L^{-1} and $C_{catalyst}$=0.1g.L^{-1}) variating the initial solution pH.
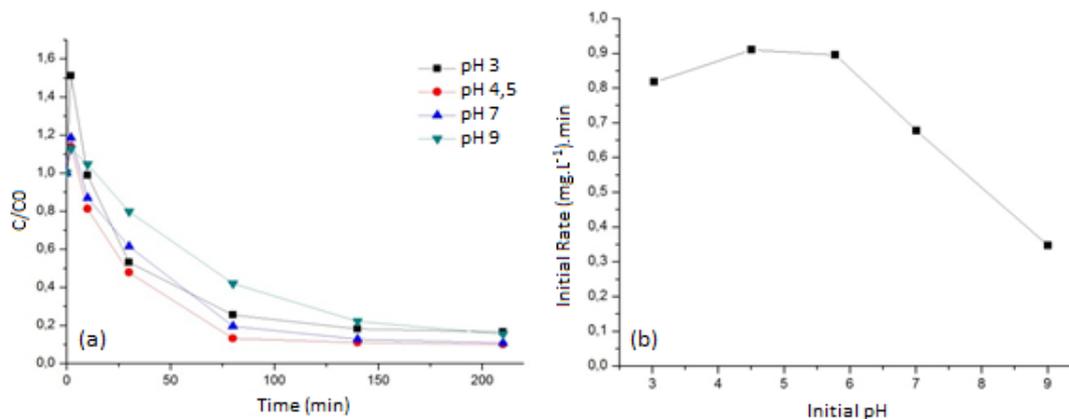
Figure 8: (a) Phenol removal for different initial pH of solution, with $0.1g.L^{-1}$ Fe_2O_3-TiO_2, $50mg.L^{-1}$ phenol and $100mg.L^{-1}$ H_2O_2 (b) initial rate of reaction *versus* initial pH of solution

It is observed in Figure 7(a) that the photo-Fenton Solar reaction with the catalyst was efficient for a wide range of pH, obtaining between 85 and 90% of Phenol removal. This result confirms that the reaction occurs with the iron in the solid phase, and not with the iron leached, since the latter, at alkaline pH, would be rapidly oxidized (Fe^{+2}/Fe^{+3}), and would precipitate, forming $Fe(OH)_3$.

A lighter color in pH=9 solution was observed because the formation of intermediates was slower. After a few minutes of reaction the coloration at pH=9 also changes to a darker brown/yellowish, there is a good removal, but with a lower speed.

The initial reaction velocity, as seen in Figure 8(b), is higher in acidic pH, between 4.5 and 6.0. This can be related to the protonation of the mixed oxide surface, with the formation of the $\equiv Fe(H_2O)_5(OH)^{+2}$ species, which through the solar irradiation results in the photo-reduction of Fe^{+3}/Fe^{+2}, with an additional generation of $^{\cdot}OH$ (ZAZO *et al.*, 2005)

3.3.3 Influence of catalyst concentration

For this experiment, the concentration of H_2O_2 used was 100 mg.L^{-1}, phenol 50 mg.L^{-1}, the pH of the solution was 6 and the concentration of the catalyst was varied from 0.025 g.L^{-1} and 0.125 g.L^{-1}. The absorption spectra are shown in Figure 9 and the degradation kinetics for the different concentrations evaluated in Figure 10. It is observed in Figure 10(a) that, for catalyst concentrations greater than 0.05g.L^{-1}, there is a rapid formation of the intermediates (starting point of the kinetic curve - $C/C_0>1.0$), 90% of phenol is removed in 120min and the initial reaction velocity, Figure 10(b), is between 0.8 and 1.0 (mg.L^{-1}) min^{-1}. For low catalyst concentration (0.025g.L^{-1}), the reaction rate is drastically reduced to 0.05 (mg.L^{-1})min^{-1}. Regardless, at the end of the process, 80% removal of phenol is obtained. This is an indication that at low catalyst concentrations, the adsorption of phenol and the formation of the intermediates, retards the reaction.
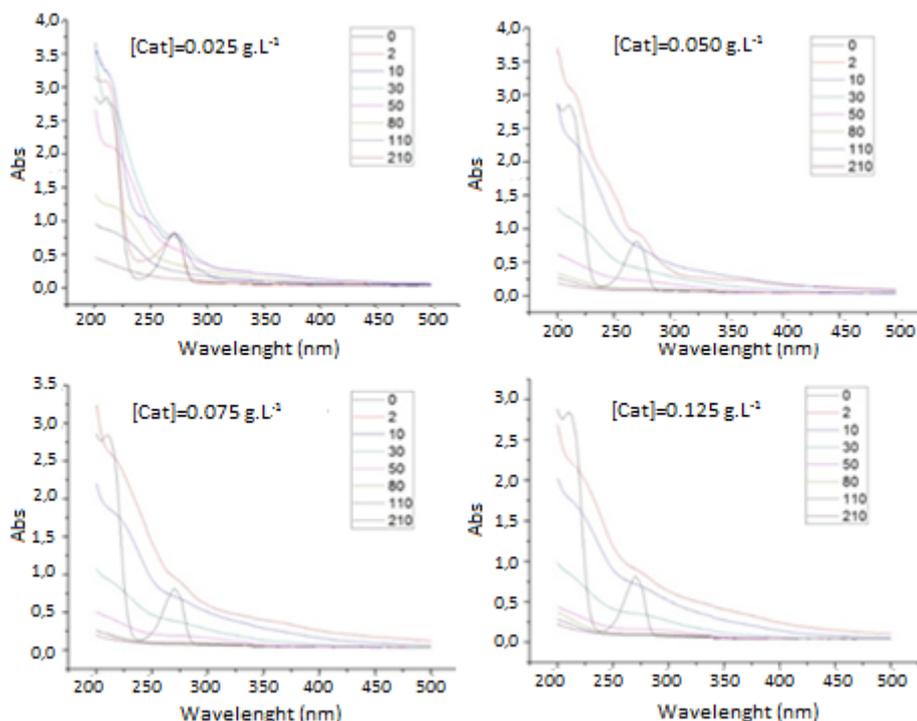
Figure 9: Degradation phenol efficiency at different catalyst concentrations.
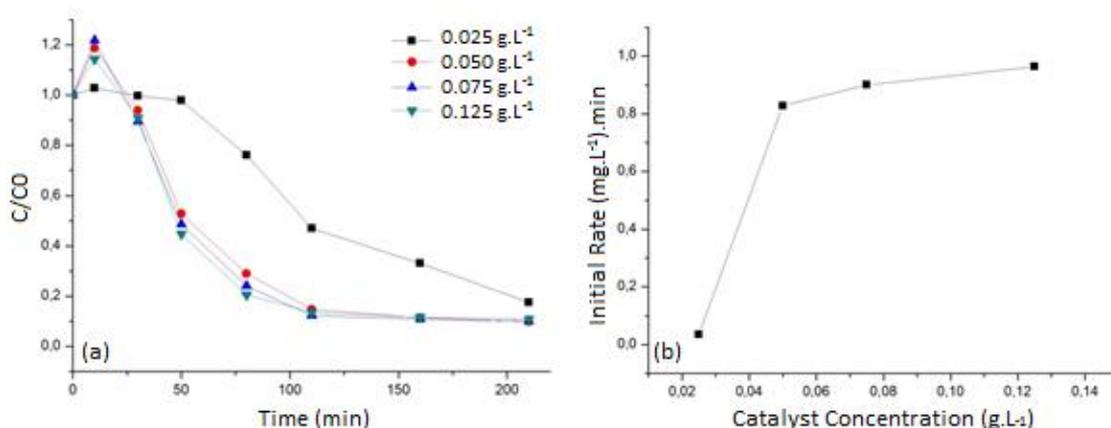
Figure 10: (a) Phenol removal for different Fe_2O_3-TiO_2 concentrations, with 50mg.L^{-1} phenol, 100mg.L^{-1} H_2O_2 and initial pH=6 and (b) initial rate of reaction *versus* catalyst concentration

3.3.4 Influence of Phenol concentration

The phenol concentration was varied from 25 mg.L^{-1} to 200 mg.L^{-1}, using a concentration of H_2O_2 of 100 mg.L^{-1}, catalyst of 0.05 g.L^{-1} and pH=6. It is observed in Figure 11(a) that for low phenol concentrations (<100 mg.L^{-1}), 80% degradation was obtained in approximately 50min of reaction. For higher phenol concentrations ($\geq$100 mg.L^{-1}), the intermediates are formed, however, they are not degraded. At the Figure 11(b) and (c) it can be observed this behavior. The complete mineralization of the phenol passes through the formation of intermediates (benzoquinone and hydroquinone), and from these, by consecutive attacks of $^{\bullet}$OH, polycarboxylic acids, CO, and H_2O are generated (SARAVANAN *et al.*, 2009).

767
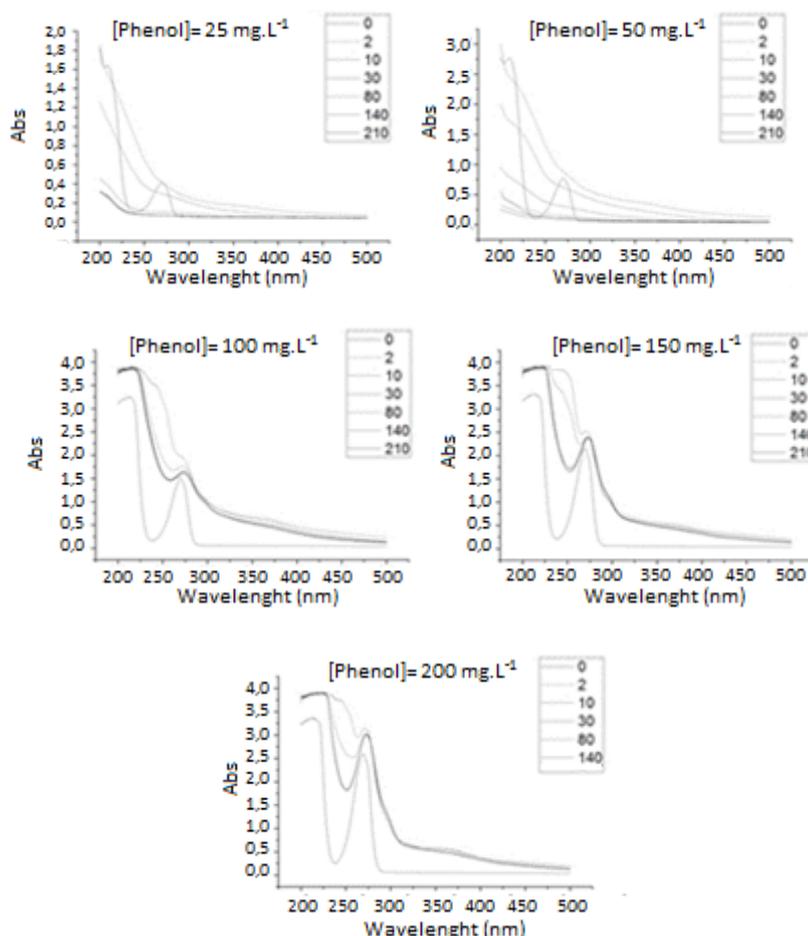
Figure 11: Absorption spectra of phenol solutions during the phenol variation test (C_{H2O2}=100mg/L; $C_{catalyst}$=0.050g/L e pH$\cong$6), with different phenol concentrations.

The influence of the solar irradiation on the photo-Fenton reaction can be observed in Table 1. Experiments were carried out under the same conditions, but on different days. It is observed that at a day with high incidence of solar irradiation (2941 KJ.m^{-2}), the highest rates of phenol degradation were obtained - 93% of removal; with the shortest reaction time - 50min, and the highest initial rate of reaction - 0.89 (mg.L^{-1})min^1.

Table 1: Influence of the solar irradiation on the reaction. The solar irradiation data are provided by The National Institute of Meteorology of Brazil, INMET, and they can be accessed at www.inmet.gov.br.

$-r_i$ ((mg.L^{-1})min^{-1})	Phenol (mg.L^{-1})	H_2O_2 (mg.L^{-1})	Solar irradiation (kJ.m^{-2})	Fe_2O_3-TiO_2 (g.L^{-1})	% removal	Time (min)
0.67	50	100	2779	0.1	89	140
0.89	50	100	2941	0.1	93	+/-50
0.72	50	100	2791	0.1	91	110

3.4 Possible mechanism for the heterogeneous photo-Fenton reaction

Adsorption of H_2O_2 at the mixed oxide active sites (S is the Fe^{+3}/Ti mixed oxide particle):

$$H_2O_2 + S \rightarrow H_2O_2.S$$
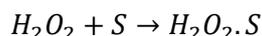
Surface reaction between adsorbed H_2O_2 and Fe^{+3} in the solid phase, generating Fe^{+2} in the solid and superoxide radical (adsorbed):

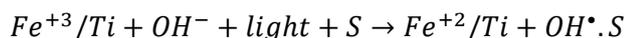$$H_2O_2.S + Fe^{+3}/Ti \rightarrow Fe^{+2}/Ti + H^+ + OOH^\bullet.S$$
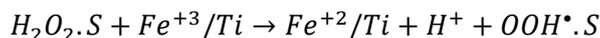
Surface reaction between adsorbed H_2O_2 and superoxide radical, also adsorbed, generating hydroxyl radical:

$$OOH^\bullet.S + H_2O_2.S \rightarrow O_2 + H_2O + OH^\bullet.S + H^+$$
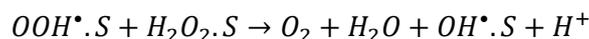
Surface reaction between the Fe^{+2} of the mixed oxide and the adsorbed H_2O_2, generating hydroxyl radical (Fenton Heterogeneous):

$$Fe^{+2}/Ti + H_2O_2.S \rightarrow Fe^{+3}/Ti + OH^- + OH^\bullet.S$$

Photreduction of Fe^{+3} into the light-activated solid, generating $OH^\bullet$ in the solid (Photo-fenton):

$$Fe^{+3}/Ti + OH^- + light + S \rightarrow Fe^{+2}/Ti + OH^\bullet.S$$

Surface reaction between the Fe^{+2} generated in the solid and the O_2 dissolved in the medium to form superoxide ion:

$$Fe^{+2}/Ti + O_2 \rightarrow O_2^{-\bullet}.S$$
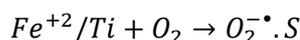
Surface reaction between the superoxide ion, adsorbed on Fe^{+3}, and the H_2O_2 adsorbed generating hydroxyl radical:

$$O_2^{-\bullet}.S + H_2O_2.S \rightarrow S + O_2 + OH^- + OH^\bullet.S$$
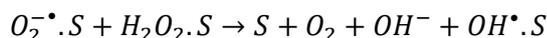
Reduced iron (Fe^{+2}) generation by the activation of sunlight gives the reduction of Fe^{+3} to Fe^{+2}:

$$Fe^{+3}/Ti + light \rightarrow Fe^{+3}/Ti(h^+, e^-) \rightarrow Fe^{+2}/Ti(h^+)$$
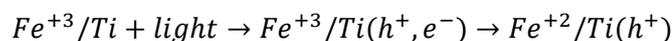
3.4.1 Undesired reactions

Surface reaction between the adsorbed H_2O_2 and the hydroxyl radical, generating superoxide radical.

$$OH^\bullet.S + H_2O_2.S \rightarrow H_2O + S + OOH^\bullet.S$$
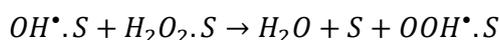
Surface reaction between two adjacent hydroxyl radicals, generating hydrogen peroxide:

$$OH^\bullet + OH^\bullet \rightarrow H_2O_2$$

769

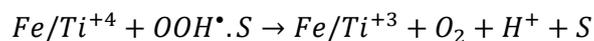Surface reaction between adsorbed superoxide radical and Fe^{+3} in the solid:

$$Fe^{+3}/Ti + OOH^{\bullet}.S \rightarrow Fe^{+2}/Ti + O_2 + H^{+} + S$$
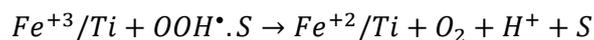
Surface reaction between adsorbed superoxide radical and Ti^{+4} in the solid:

$$Fe/Ti^{+4} + OOH^{\bullet}.S \rightarrow Fe/Ti^{+3} + O_2 + H^{+} + S$$

4. Conclusions

A Fe_2O_3-TiO_2 catalyst was produced at the proportion 60:40 (%mass) for its use in a photo-Fenton solar process. According to the results shown it is possible to conclude that for the following conditions: (1) phenol concentration$\leq$50mg.L^{-1}; (2) $H_2O_2\geq$100mg.L^{-1} and (3) catalyst$\geq$0.05g.L^{-1}, the rate of reaction is independent of these parameters and its kinetics constant is between 1.0 and 0.9 (mg.L^{-1}) min^{-1}, with a strong dependence on solar irradiation and more than 90% of phenol removal can be achieved. Therefore, there was a positive interaction between Fe and Ti in an effort to produce hydroxyl radical, hence the degradation of the pollutant.

References

AKHAVAN, O., AZIMIRAD, R. 2009. Photocatalytic property of Fe_2O_3 nanogran chains coated by TiO_2 nanolayer in visible light irradiantion. Applied Catalysis A: General 369:77-82. https://doi.org/10.1016/j.apcata.2009.09.001.

AMBATI, R., COGATE, P. R. 2017. Photocatalytis degradation of Acid Blue 80 using iron doped TiO_2 catalyst: Understanding the effect of operating parameters and combinations for synergism. Journal of Water Process Engineering 20:217-225. https://doi.org/10.1016/j.jwpe.2017.11.005

BOKARE, A. D., CHOI, W. 2014. Review of iron-free fenton-like systems for activating H_2O_2 in Advanced oxidation Processes, journal of Hazardous Materials 275:121-135. https://doi.org/10.1016/j.jhazmat.2014.04.054

CONG, Y., LI, Z., ZHANG, Y., WANG, Q., XU, Q. 2012. Synthesis of α-Fe_2O_3/TiO_2 nanotube arrays for photoelectro-Fenton degradation of phenol. Chemical Engineering Journal 191:356–363. https://doi.org/10.1016/j.cej.2012.03.031

DOUMIC, L. I., SOARES, P. A., AYUDE, M. A., CASSANELLO, M., BOAVENTURA, R. A. R., VILAR, V. J. P. 2015. Enhancement of a solar photo-Fenton reaction by using ferrioxalate complexes for the treatment of a synthetic cotton-textile dyeing wastewater. Chemical Engineering Journal 277:86-96. https://doi.org/10.1016/j.cej.2015.04.074.

DU, Y., ZHAO, L., ZHANG, Y. 2014. Roles of TaON and Ta_3N_5 in the visible-Fenton-like degradation of atrazine. Journal of Hazardous Materials 276:55-61. https://doi.org/10.1016/j.jhazmat.2013.12.042

LIANG, C., LIU, Y., LI, K., XING, S., MA, Z., WU, Y. 2017. Heterogeneous photo-Fenton degradation of organic pollutants with amorphous Fe-Zn-oxide/hydrochar under visible light irradiation. Separation and Purification Technology 188:105-111. https://doi.org/10.1016/j.seppur.2017.07.027.

LI, J., LIU, Z., WANG, D., ZHU, Z. 2014. Materials Science in Semiconductor processing 27: 950-957. Visible-light responsive carbon-anatase-hematite core-shell microspheres for methylene blue photodegradation. https://doi.org/10.1016/j.mssp.2014.08.038.

M. P. Pechini, *US Patent 3.330.697* (1967).

MAHADIK, M. A., SHINDE, S. S., MOHITE, V. S., KUMBHAR, S. S., MOHOLKAR, A. V., RAJPURE, K. Y., GANESAN, V., NAYAK, J., BARMAN, S. R., BHOSALE, C. H. 2014. Visible light catalysis of rhodamine B using nanostructures Fe_2O_3, TiO_2 and $TiO_2/Fe2O_3$ thin films. Journal of Photochemstry and Photobiology B: Biology 133: 90-98. https://doi.org/10.1016/j.jphotobiol.2014.01.017.

MENDONÇA, V. R., LOPES, O. F., FREGONESI, R. P., GIRALDI, T. R., RIBEIRO, C. 2014. TiO2-SnO2 heterostructures applied to dye photodegradation: The relationship between variables of synthesis and photocatalytic performance. Applied Surface Science 298:182-191. https://doi.org/10.1016/j.apsusc.2014.01.157

MISHRA, M., CHUN, D. 2015. α-Fe_2O_3 as a photocatalytic material: A review. Applied Catalysis A: General 498:126-141. https://doi.org/10.1016/j.apcata.2015.03.023

PENG, L., XIE, T., LU, Y., FAN, H., WANG, G. 2010. Synthesis, photoelectric properties and photocatalytic activity of the Fe_2O_3/TiO_2 heterogeneous photocatalysts. Physical Chemistry Chemical Physics 12:8033-8041

SARAVANAN, P., PAKSHIRAJAN, K., SAHA, P. 2009. Degradation of phenol by TiO_2-based heterogeneous photocatalysts in presence of sunlight. Journal of Hydro-environment Research 3:45-50.

VIRARAGHAVAN, T., ALFARO, F. L. 1998. Adsorption of phenol from wastewater by peat, fly ash and bentonite. Journal of Hazardous Materials 57: 59-70. https://doi.org/10.1016/S0304-3894(97)00062-9

XU, P., ZENG, G. M., HUANG, D. L., FENG, C. L., HU, S., ZHAO, M. H., LAI, C., WEI, Z., HUANG, C., XIE, G. X., LIU, Z. F. 2012. Use of iron oxide nanomaterials in wastewater treatment: A review. Science of The Total Environment 424:1-10. https://doi.org/10.1016/j.scitotenv.2012.02.023

ZAZO, J. A., CASAS, J. A., MOHEDANO, A. F., GILARRANZ, M. A., RODRÍGUEZ, J. J. 2005. Chemical pathway and kinetics of phenol oxidation by Fenton's reagent. Environmental Science and Technology 1;39(23):9295-302.

ZENG, G. M., LI, X., HUANG, J. H., ZHANG, C., ZHOU, C. F., NIU, J., SHI, L. J., ELE, S. B., LI, F. 2011. Micellar-enhanced ultrafiltration of cadmium and methylene blue in synthetic wastewater using SDS. J Hazard 185(2–3):1304–10.